The Astrophysical Journal Letters, 800:L32 (7pp), 2015 February 20 doi:10.1088/2041-8205/800/2/L32

THE IMPRINTS OF THE GALACTIC BAR ON THE THICK DISK WITH RAVE

T. Antoja[1,2,15], G. Monari[2,3], A. Helmi[2], O. Bienaymé[3], J. Bland-Hawthorn[4], B. Famaey[3], B. K. Gibson[5], E. K. Grebel[6], G. Kordopatis[7], U. Munari[8], J. Navarro[9], Q. Parker[10,11,12], W. A. Reid[11], G. Seabroke[13], M. Steinmetz[7], and T. Zwitter[14]
[1] Scientific Support Office, Directorate of Science and Robotic Exploration, European Space Research and Technology Centre (ESA/ESTEC), Keplerlaan 1, NL-2201 AZ Noordwijk, The Netherlands; tantoja@cosmos.esa.int
[2] Kapteyn Astronomical Institute, University of Groningen, P.O. Box 800, NL-9700 AV Groningen, The Netherlands
[3] Observatoire Astronomique de Strasbourg, Université de Strasbourg, CNRS, UMR 7550, 11 rue de l'Université, F-67000 Strasbourg, France
[4] Sydney Institute for Astronomy, School of Physics A28, University of Sydney, Sydney, NSW 2006, Australia
[5] Jeremiah Horrocks Institute, University of Central Lancashire, Preston PR1 2HE, UK
[6] Astronomisches Rechen-Institut, Zentrum für Astronomie der Universität Heidelberg, Mönchhofstr.12-14, D-69120 Heidelberg, Germany
[7] Leibniz-Institut für Astrophysik Potsdam (AIP), An der Sternwarte 16, D-14482 Potsdam, Germany
[8] INAF Osservatorio Astronomico di Padova, I-36012 Asiago (VI), Italy
[9] University of Victoria, Victoria, BC V8P 5C2, Canada
[10] Research Centre in Astronomy, Astrophysics and Astrophotonics, Macquarie University, Sydney, NSW 2109, Australia
[11] Department of Physics and Astronomy, Macquarie University, Sydney, NSW 2109, Australia
[12] Australian Astronomical Observatory, P.O. Box 915, North Ryde, NSW 1670, Australia
[13] Mullard Space Science Laboratory, University College London, Holmbury St Mary, Dorking RH5 6NT, UK
[14] Faculty of Mathematics and Physics, University of Ljubljana, Jadranska 19, 1000 Ljubljana, Slovenia
Received 2014 December 17; accepted 2015 January 26; published 2015 February 20

ABSTRACT

We study the kinematics of a local sample of stars, located within a cylinder of 500 pc radius centered on the Sun, in the RAVE data set. We find clear asymmetries in the v_R - v_ϕ velocity distributions of thin and thick disk stars: there are more stars moving radially outward for low azimuthal velocities and more radially inward for high azimuthal velocities. Such asymmetries have been previously reported for the thin disk as being due to the Galactic bar, but this is the first time that the same type of structures are seen in the thick disk. Our findings imply that the velocities of thick-disk stars should no longer be described by Schwarzschild's, multivariate Gaussian or purely axisymmetric distributions. Furthermore, the nature of previously reported substructures in the thick disk needs to be revisited as these could be associated with dynamical resonances rather than to accretion events. It is clear that dynamical models of the Galaxy must fit the 3D velocity distributions of the disks, rather than the projected 1D, if we are to understand the Galaxy fully.

Key words: Galaxy: disk – Galaxy: kinematics and dynamics – Galaxy: structure

1. INTRODUCTION

The velocity distribution of stars in the solar neighborhood contains key information about the current dynamical state of our Galaxy and also about its history. The kinematics of stars can be used to derive both the mass distribution of the Milky Way through sophisticated dynamical models, as well as to identify accretion events.

The velocities of thin-disk stars are often described by the Schwarzschild distribution function, which considers each of the velocity components separately. However, data from the *Hipparcos* mission (Perryman et al. 1997) and later from the Geneva–Copenhagen survey (Holmberg et al. 2009) have revealed a more complex distribution with significant overdensities and structure (Dehnen 1998; Famaey et al. 2005; Antoja et al. 2008). Some of the overdensities and distortions of the velocity distribution appear to be the imprints of the non-axisymmetric components of the Milky Way, namely, the spiral arms and Galactic bar (e.g., Dehnen 2000; De Simone et al. 2004; Sellwood 2010; Antoja et al. 2011; McMillan 2011). Streams or moving groups are formed by stars on orbits that are close to resonant with the natural frequencies of the spiral arms and/or the bar. Examples of such moving groups that are heterogeneous in age and chemical composition are the Pleiades, Hyades, Sirius, and Hercules streams (the latter very likely driven by the bar).

On the other hand, the velocity distribution of the thick disk has been studied in less detail thus far because of limitations in the size of volume complete samples. In practice, this has implied that Gaussian distributions were used to fit the kinematics of thick-disk stars (see Binney et al. 2014b and Sharma et al. 2014 for a recent discussion on how Gaussian functions poorly fit all velocity components). Furthermore, substructures have also been reported in the thick disk (e.g., Gilmore et al. 2002; Navarro et al. 2004; Helmi et al. 2006), identified through statistical comparisons with Galactic models or with simple kinematic models such as those discussed above.

Many of these substructures have been attributed to accretion events, as these typically leave behind streams of stars with similar velocities that do not necessarily appear to be spatially coherent near the Sun because of the short mixing timescales in the inner Galaxy. However, recent modeling has shown that the impact of spiral arms (Solway et al. 2012; Faure et al. 2014) and the Galactic bar on the kinematics of stars in the thick disk is non-negligible. For example, Monari et al. (2013) and Monari (2014) have found in their simulations that there is as much resonant trapping in the thick disk as in the thin disk. Another clear signature of the impact of the bar in their thick-disk simulations is a bimodality in the velocity distribution for stars located near the Outer Lindblad Resonance, similar to that observed in the thin disk.

[15] ESA Research Fellow.

Here we explore whether these features are present in local samples of thick-disk stars, especially now that such samples have increased in size by large factors (as in, e.g., LAMOST and SEGUE; Cui et al. 2012 and Yanny et al. 2009, respectively). For example the Geneva–Copenhagen survey contained ~17,000 stars, while ~400,000 stars have now been measured by the RAdial Velocity Experiment (RAVE; Steinmetz et al. 2006). We report on the analysis of the *local* RAVE data set and indeed find clear asymmetries/structures in the velocity distributions of local thick-disk stars, which can be attributed to the resonant interaction with the Galactic bar. In Section 2, we present the data set and the selection of the different populations; in Section 3, we provide the analysis; and we conclude in Section 4 with a discussion on the implications of our findings.

2. OBSERVATIONS AND DATA SELECTION

In this study, we use the RAVE Data Release 4 (DR4; Kordopatis et al. 2013b). The stellar atmospheric parameters of the DR4 are computed using two different pipelines, presented by Kordopatis et al. (2011) and Siebert et al. (2011). The stellar parallaxes that we use were obtained through the Bayesian distance-finding method of Binney et al. (2014a).

First, we select stars with (i) a signal-to-noise ratio better than 20, (ii) the first morphological flag indicating that they are normal stars (Matijevič et al. 2012), and (iii) the converged algorithm of computation of the physical parameters. From these, we further select those in a cylinder with a radius of 500 pc centered on the Sun's position. This results in a sample of 162,153 stars with 6D phase-space information, of which 76% are dwarf stars and 24% are giants. The DR4 proper motions were compiled from several catalogs, and here we use UCAC4 (Zacharias et al. 2013).

Following Reid et al. (2014), we assume that the Sun is at $X = -8.34$ kpc and take a circular velocity at the Sun of $V_0 = 240$ km s^{-1}. For the velocity of the Sun with respect to the Local Standard of Rest, we adopt $(U_\odot, V_\odot, W_\odot) = (10, 12, 7)$ km s^{-1} (Schönrich et al. 2010). The resulting value of $(V_0 + V_\odot)/R_0$ is 30.2 km s^{-1} kpc^{-1}, which is compatible with that from the reflex motion of Sgr A* 30.2 ± 0.2 km s^{-1} kpc^{-1} (Reid & Brunthaler 2004). With these values, we compute the stars' cylindrical velocities: v_R (positive toward the Galactic center, in consonance with the usual U velocity component) and v_ϕ (toward the direction of rotation).

From the selected sample, we consider four different subsets of stars based on their height and their metallicity to maximize or minimize the number of thin- or thick-disk stars. The properties of each subset and relative thin/thick/halo fractions are listed in Table 1. Two of the subsets are located on the plane but have metallicities corresponding to thin-disk (1) and to thick-disk (3) components, respectively. The other two are located far from the plane and have intermediate (2) and low (4) metallicities and could be both associated with the thick disk.

For each subset, it is important to estimate the fraction of stars that could belong to a different population than desired. We have derived two different estimates of these fractions for each of the samples. The first estimate, which we term RAVE-fit, is based on an admittedly simplistic three-Gaussian population model (old thin disk, thick disk, and halo) fit to the metallicity distribution to RAVE data by Kordopatis et al. (2013a, their Tables 1 and 2). We use the fits derived for *all* stars with galactocentric radius between 7.5 and 8.5 kpc to estimate the population fraction for samples (1) and (3). Since these samples have an additional constraint, namely, $|Z| \leqslant 0.5$ kpc, the fractions of thick-disk and halo stars are probably overestimated. For samples (2) and (4), we use the RAVE fits derived for stars $1 < |Z| < 2$ kpc in the same radial range. In this case, since in our samples we consider all stars with $|Z| > 0.5$ kpc, it is likely that the fraction of thin- and thick-disk stars is underestimated, while that of the halo is overestimated. In fact, if we assume that the halo has no net rotation and that all stars with $v_\phi < 0$ belong to the halo, we can estimate the fraction of halo stars as twice that of stars with $v_\phi < 0$. We find this to be of only 3%, 0.7%, and 4% for samples (2), (3), and (4), respectively, i.e., much smaller than the fractions obtained through the RAVE-fit.

The second estimate (fit 2) of the contamination in our subsets is based on a simple model with two populations (thin and thick disk) with specified density and metallicity distributions. We use two exponential disks with vertical scale heights[16] of $h_{z,\mathrm{thin}} = 0.3$ kpc and $h_{z,\mathrm{thick}} = 0.9$ kpc and scale lengths of $h_{R,\mathrm{thin}} = 2.6$ kpc and $h_{R,\mathrm{thick}} = 3.6$ kpc, and a local density normalization of 12%, all as measured by Jurić et al. (2008).[17] We also assume Gaussian metallicity distributions with means $\langle\, [\mathrm{M/H}]_{\mathrm{thin}} \,\rangle = -0.1$ and $\langle\, [\mathrm{M/H}]_{\mathrm{thick}} \,\rangle = -0.78$ and dispersions $\sigma_{\,[\mathrm{M/H}]_{\mathrm{thin}}} = 0.2$ and $\sigma_{\,[\mathrm{M/H}]_{\mathrm{thick}}} = 0.3$ (similar to the intermediate old thin- and thick-disk populations of Robin et al. 2003, respectively). We estimate the fraction of each population by integrating between the given ranges of metallicities and heights. For samples (2) and (4), we assume a maximum height of 1.5 kpc.

The population fractions estimated with the two methods (RAVE-fit and fit 2) indicate that the contamination of thick-disk stars in sample (1) is very low. On the other hand, samples (2)–(4) are clearly dominated by the thick disk as desired.

3. STATISTICAL ANALYSIS

In Figure 1, we show the velocity distributions of the different samples using scatter plots (left) and a kernel density estimator (right; see the caption for details). The velocity distribution of the thin disk, subset (1), is not homogeneous and depicts overdensities and asymmetries, as already reported in Antoja et al. (2012) for RAVE thin-disk stars. We see a clear asymmetry: stars with $v_\phi \lesssim 220$ km s^{-1} are shifted to the left part of the distribution ($v_R < 0$). Interestingly, this asymmetry is visible in the thick-disk subsets for both scatter and density plots shown in the remaining panels.

To study this in more detail, we use the density field shown in the right panels of Figure 1 to compute the difference between regions with positive and negative v_R. In practice, if σ_+ is the density in a certain pixel (v_R, v_ϕ) of the grid (of 2 km s^{-1} size) and σ_- is the number for the symmetric pixel $(-v_R, v_\phi)$, we compute $\Delta = \sigma_+ - \sigma_-$. This quantity is plotted in Figure 2. Red colors indicate $\Delta > 0$ (more stars with $v_R > 0$), and blue colors $\Delta < 0$.

[16] The scale lengths and density normalization of the disks are uncertain (see, e.g., Bensby et al. 2011).

[17] Robin et al. (2003) give a normalization of 27% for the intermediate age to old thin to thick disk. This would yield an even lower thin-disk contamination in samples (2)–(4).

Table 1
Properties of the Different Cuts

			N	e_Z (kpc)	$e_{\mathrm{dist}_{2d}}$ (kpc)	e_{v_R} (km s^{-1})	e_{v_ϕ} (km s^{-1})	e_{v_Z} (km s^{-1})	$e_{\mathrm{[M/H]}}$ (dex)	RAVE-fit (Thin)	RAVE-fit (Thick)	RAVE-fit (Halo)	Fit 2 (Thin)	Fit 2 (Thick)
1	[M/H] $\geqslant -0.1$ dex	$\lvert Z\rvert \leqslant 0.5$ kpc	47,883	0.05	0.05	5.0	4.3	3.3	0.10	96	4	0.5	99.8	0.2
2	[M/H] < -0.45 dex	$\lvert Z\rvert > 0.5$ kpc	5123	0.38	0.13	15.7	15.1	5.2	0.10	0.2	88	11	13	87
3	[M/H] < -0.7 dex	$\lvert Z\rvert \leqslant 0.5$ kpc	21,624	0.06	0.06	6.6	5.0	4.0	0.12	0.7	78	22	3	97
4	[M/H] < -0.7 dex	$\lvert Z\rvert > 0.5$ kpc	2939	0.40	0.13	17.3	18.0	5.4	0.10	0.003	68	32	0.7	99.3

Note. The first columns show the cuts, the number of stars N, median errors in vertical position Z, in horizontal distance in the plane from the Sun dist_{2d}, in the velocity components (v_R, v_ϕ and v_Z), and in the metallicity [M/H]. The last five columns show the thin disk, thick disk, and halo fraction of stars computed according to different models (named RAVE-fit and fit 2; see the text for caveats with respect to the estimated halo fraction).

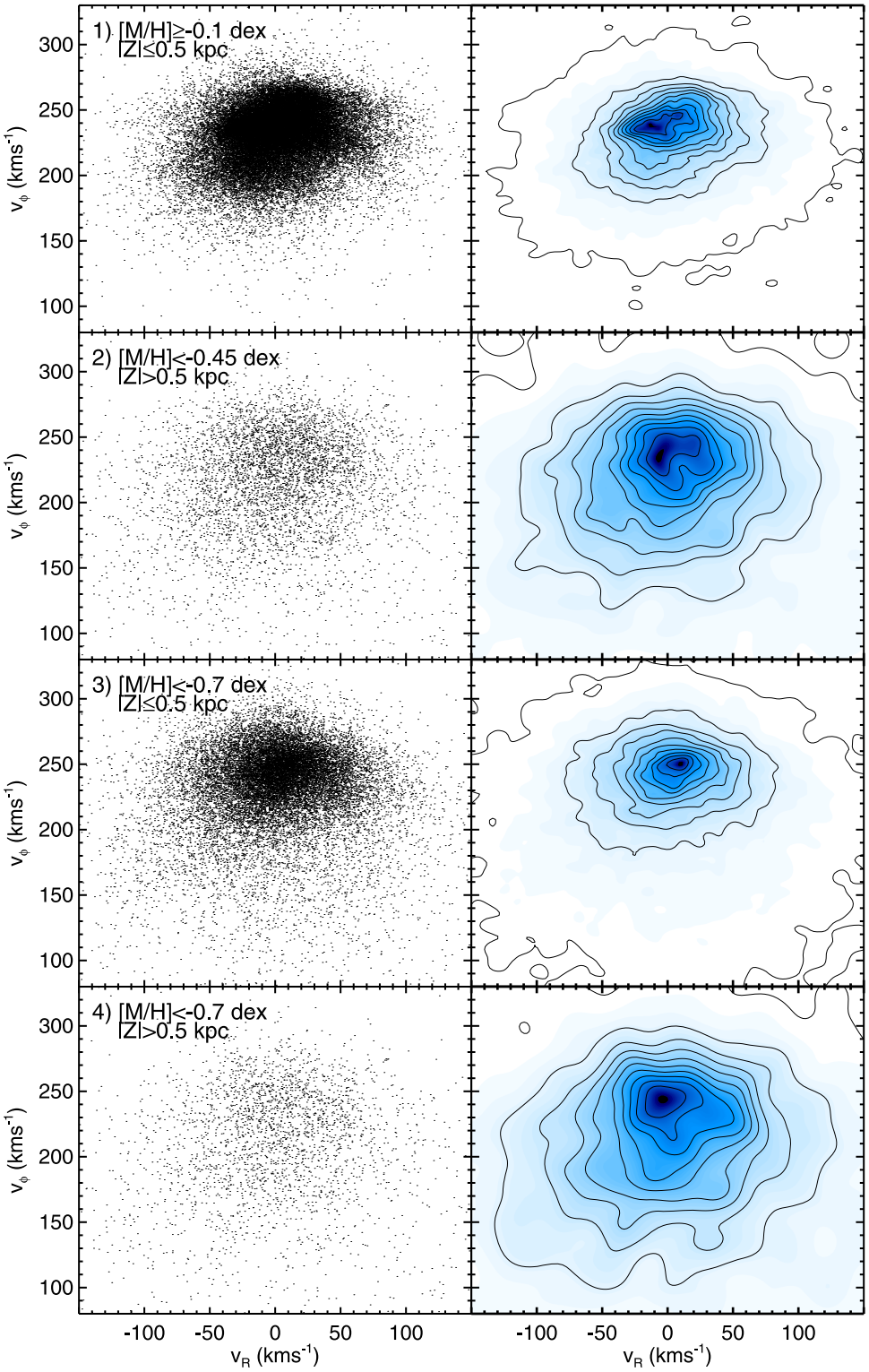

Figure 1. Velocities of stars in the different cuts of the RAVE data set of Table 1. Left column: scatter plots. Right column: density obtained through the Epanechnikov adaptive kernel density estimator method (Silverman 1986) with an adaptability exponent of 0.1. The density was estimated in a uniform grid of 2 km s^{-1}. The black contours indicate the following levels in units of the maximum density: 0.005, 0.1, 0.2, 0.3, 0.4, 0.5, 0.6, 0.7, 0.8, 0.9, 0.995.

The upper left panel in Figure 2, corresponding to the thin-disk sample, clearly shows that the region with $v_\phi \gtrsim 240$ km s^{-1} has an excess of stars with $v_R > 0$, while the contrary is true for $v_\phi \lesssim 240$ km s^{-1}. This separation is not at constant v_ϕ for all v_R (i.e., horizontal in the v_R - v_ϕ diagram), but rather varies with v_R. The other three panels, corresponding to the thick-disk subsets, depict a similar asymmetry. However, in these cases, the asymmetry is not as sharp and clear as for the thin-disk set. This is probably due to the larger velocity errors and to the lower number of stars, especially for samples (2) and (4). Nevertheless, the asymmetry is very clear for sample (3), and it is located roughly at the same velocities as for sample (1). Despite limitations for samples (2) and (4), it is still clear

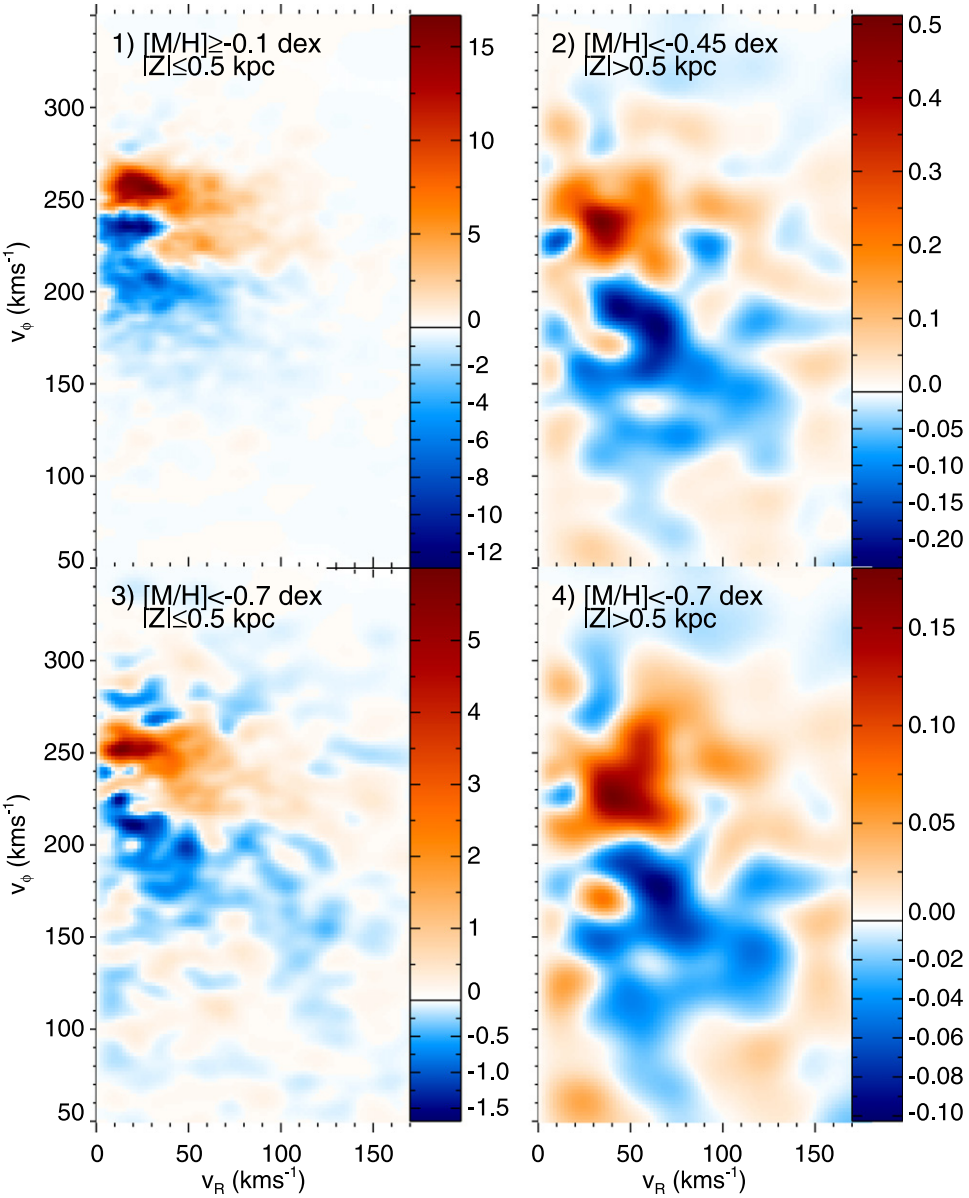

Figure 2. Differences in the density field (depicted in the right panels of Figure 1) for stars with positive and negative v_R for the different subsets. The density was normalized to the number of stars in each sample, and therefore the color bars indicate the difference in the number of stars in each pixel of the grid (of 2 km s^{-1}).

that red colors dominate the upper half of the distribution, while blue colors dominate in the other half.[18]

The left panel of Figure 3 is a one-dimensional (1D) version of Figure 2, where we plot for each v_ϕ the difference between the counts for $v_R > 0$ (N_+) and those for $v_R < 0$ (N_-). We use the method presented in Scargle et al. (2013) and implemented in VanderPlas et al. (2012) to bin the data in v_ϕ. It is a non-parametric technique that finds the optimal data segments of variable size that maximize a certain fitness function in a Bayesian likelihood framework and are based on Poissonian statistics. Although the binning choice is arbitrary, we have checked that our conclusions do not change if we use bins of equal size or bins with an equal number of stars. For this figure, we plot also in red (right vertical axis) the relative asymmetry in the counts, i.e., $\tilde{\Delta} = (N_+ - N_-)/(N_+ + N_-)$.

This plot shows the trend already highlighted in the two-dimensional plots of Figure 2. There is a large asymmetry in the counts toward $v_R > 0$ that peaks at $v_\phi \sim 230-250$ km s^{-1} and extends from $v_\phi \sim 200$ to $\sim$275 km s^{-1}. A smaller but significant (note the small errors) asymmetry $\Delta < 0$ is detected for velocities below $\sim$200 km s^{-1} and at least down to 120−140 km s^{-1}. This asymmetry is in a region of the velocity plane with a lower number of stars and is thus better seen for the red curves that correspond to the normalized counts $\tilde{\Delta}$.

In the right panel of Figure 3, we show the mean v_R as function of v_ϕ for all the subsets using the same binning as before. The shape of these curves is similar to those on the left plot. This is because an excess of counts for positive v_R reflects in a positive mean v_R and conversely. The change in sign of the mean v_R is significant for all four samples and occurs at $v_\phi \sim 200-220$ km s^{-1}. It is noteworthy that the negative

[18] Note that a wrong assumption of the peculiar velocity of the Sun $U_\odot$ would also produce an asymmetry in the counts of $v_R > 0$ with respect to $v_R < 0$, but this would be positive or negative everywhere and would not depend on v_ϕ as we see here. Note also that a different assumption of the values for R_0, $V_\odot$ and V_0 cannot produce the observed asymmetries, only shifting the positions or the velocity v_ϕ.

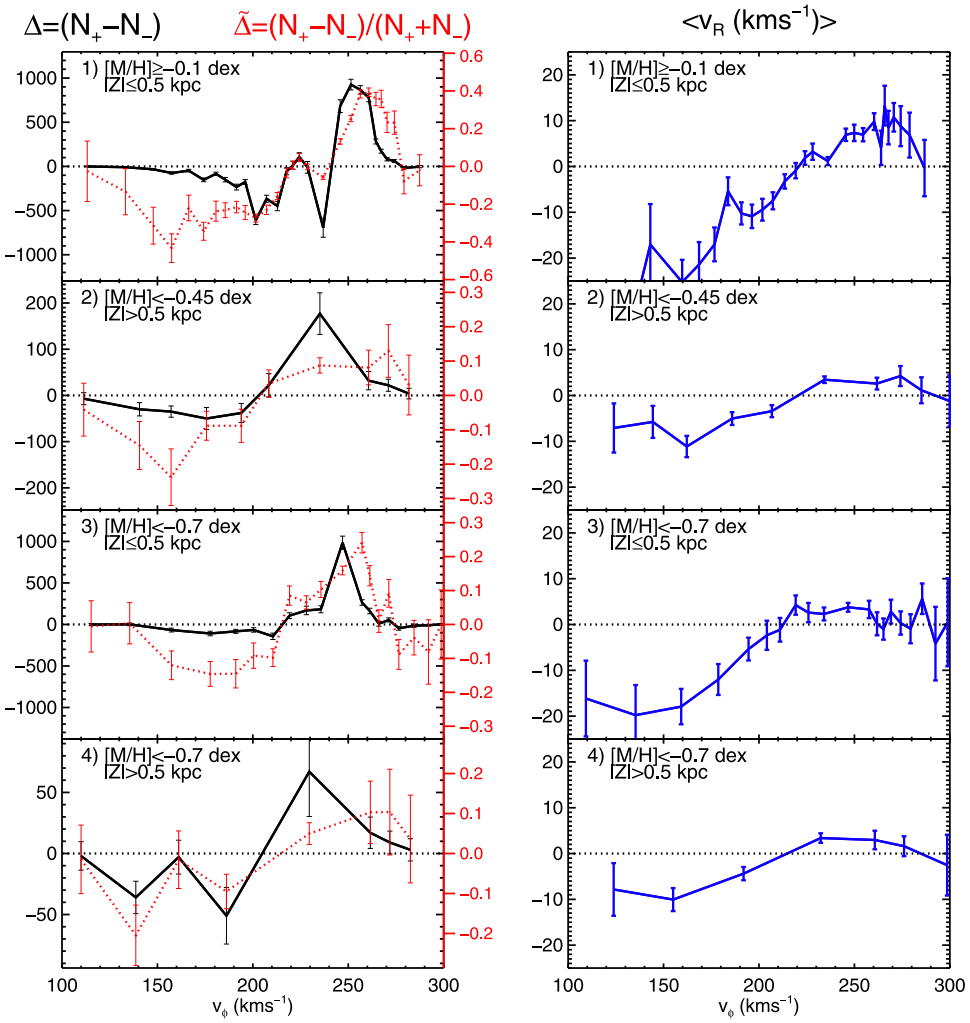

Figure 3. Left: difference in the number of counts between positive and negative v_R, $\Delta = (N_+ - N_-)$ (black curves) and the same number scaled to the total number of stars in both bins $\tilde{\Delta} = (N_+ - N_-)/(N_+ + N_-)$ (red curves, right axis) as function v_ϕ for the different subsets. Right: mean v_R velocity for bins in v_ϕ for the different samples.

asymmetry seen both in the counts and in the mean v_R extends well into low v_ϕ, a region more often thought to be characteristic of accretion events. For instance, this is where the Arcturus stream is also located (Navarro et al. 2004).

For the thin-disk sample (top panels of Figure 3), we also observe other smaller bumps and more detailed features. In particular, two clear positive peaks are seen both in the counts $\tilde{\Delta}$ and in the mean v_R. These are due to known kinematic overdensities in the solar neighborhood. Some hints of similar bumps (e.g., at $v_\phi \sim 215-220$ km s^{-1} and at $v_\phi \sim 250 - 260$ km s^{-1}) are also seen for the thick-disk sample (3).

The results presented above are robust to the specific choice of the proper motion catalog, as we have checked that no significant differences are seen when using other catalogs, namely, UCAC2 and UCAC3 (Zacharias et al. 2010 and references therein), Tycho-2 (Høg et al. 2000), and PPMXL (Roeser et al. 2010). We also obtained the same results when we scaled the distances by factors of 0.8 and 1.2, i.e., assuming that the distances were overestimated and underestimated by 20%, respectively. Furthermore, the choice of the volume of the cylinder has no effect on our results: stars with the same cuts but located in a cylindrical ring with inner and outer radii of 0.5 and 1 kpc (dominated by giant stars instead of by dwarfs as in our initial cylinder) show the same asymmetries.

As mentioned in Section 1, the main effect of the bar on the local velocity distribution is a bimodality in the velocity distribution near the Outer Lindblad Resonance (Kalnajs 1991; Dehnen 2000). This produces the Hercules stream, an excess of stars with negative v_R at velocities around $v_\phi = 190$ km s^{-1} (heliocentric velocity $V \sim -50$ km s^{-1}), and the dominant mode of low-velocity stars centered around the local standard of rest ($v_\phi = 240$ km s^{-1}) and with an elongation through positive v_R. We believe that the asymmetries that we observe have the same origin.

4. DISCUSSION AND CONCLUSIONS

We have found clear asymmetries in the v_R-v_ϕ velocity distributions of thin- and thick-disk stars near the Sun. In the thin disk, such asymmetries are due to well-known overdensities such as the Hercules stream, which has been explained by the resonant effects of the bar near its OLR.

This is the first time that the same type of structures and asymmetries are seen in the thick disk. The features are significant for the three different thick-disk samples considered based on metallicity and height above the plane, which we have estimated to have low contamination from thin-disk and halo

stars. These findings suggest that the Galactic bar leaves strong imprints on both the thin and thick disk.

It is clear that the observed v_ϕ velocities are highly skewed, not following a Gaussian distribution. Binney et al. (2014b) also showed that the radial and vertical velocities cannot be fitted by Gaussian functions, not only due to moving groups but also because they peak more sharply than Gaussians. Our results also imply that the velocities of thick-disk stars should no longer be described by independent Schwarzschild, multivariate Gaussian, or purely axisymmetric distributions: the reported asymmetry is both v_ϕ and v_R dependent. The RAVE data set has also shown peculiar vertical velocity patterns (Williams et al. 2013), and other studies based on simulations have found that the non-axisymmetries of the Galaxy can also influence the vertical velocity distribution (Faure et al. 2014). It follows that that dynamical models of the Galaxy must fit the 3D velocity distributions rather than the projected 1D.

Simulations show that the deformations and overdensities of the velocity distribution caused by the bar change with position (both in radius and azimuthal angle) in the thin (e.g., Dehnen 2000; Antoja et al. 2014) and in the thick disk as well (Monari et al. 2013). This implies that the asymmetries in the velocity distribution of the thick disk must change with spatial position. Interestingly, rotational lags and asymmetries in the thick disk were reported by Humphreys et al. (2011) and Jayaraman et al. (2013), which may be further evidence of this. Future modeling of the velocity distributions must therefore be position dependent. One should notice that the asymmetry projects differently on line of sight and transverse velocity, creating different signatures.

This also implies that the nature of previously found substructures in the thick disk needs to be revisited as these could be associated with dynamical resonances rather than with accretion events. Specifically, the Arcturus stream would seem to be naturally explained in this way, being an extension toward lower v_ϕ velocities, which would also be favored given its chemical abundances (Williams et al. 2009), and hence there would be no need to invoke any accretion events nor ringing due to a past merger event (Minchev et al. 2009). Also the substructure reported by Gilmore et al. (2002) could perhaps be explained along similar lines, although it was suggested that this is part of a metal-weak thick disk (Kordopatis et al. 2013c). The role of the bar on the formation of such structures should thus be investigated.

It is clear that with the advent of larger and more precise samples of the disk kinematics, we are entering a new era where the classic velocity distribution models are not sufficient and the effects of the non-axisymmetry in the disk have to be taken into account in the modeling. This is particularly relevant now given that in approximately two years time the first *Gaia* data will be published and we expect to detect these and perhaps other asymmetries far beyond the Sun.

T.A. is supported by an ESA Research Fellowship in Space Science. We thank Ralf Scholz for constructive comments on the analysis. A.H. was partially supported by ERC-StG GALACTICA-240271. G.M. is supported by the *Centre National d'Etudes Spatiales* (CNES). Funding for RAVE has been provided by the Anglo-Australian Observatory; the Leibniz-Institut fuer Astrophysik Potsdam; the Australian National University; the Australian Research Council; the French National Research Agency; the German Research foundation; the Istituto Nazionale di Astrofisica at Padova; The Johns Hopkins University; the National Science Foundation of the USA (AST-0908326); the W.M. Keck foundation; the Macquarie University; The Netherlands Research School for Astronomy; the Natural Sciences and Engineering Research Council of Canada; the Slovenian Research Agency; the Swiss National Science Foundation; the Science & Technology Facilities Council of the UK; Opticon; Strasbourg Observatory; and the Universities of Groningen, Heidelberg, and Sydney. The RAVE website is http://rave-survey.org. We thank the anonymous referee for helpful comments.

REFERENCES

Antoja, T., Figueras, F., Fernández, D., & Torra, J. 2008, A&A, 490, 135
Antoja, T., Figueras, F., Romero-Gómez, M., et al. 2011, MNRAS, 418, 1423
Antoja, T., Helmi, A., Bienaymé, O., et al. 2012, MNRAS, 426, L1
Antoja, T., Helmi, A., Dehnen, W., et al. 2014, A&A, 563, A60
Bensby, T., Alves-Brito, A., Oey, M. S., Yong, D., & Melendez, J. 2011, ApJL, 735, L46
Binney, J., Burnett, B., Kordopatis, G., et al. 2014a, MNRAS, 437, 351
Binney, J., Burnett, B., Kordopatis, G., et al. 2014b, MNRAS, 439, 1231
Cui, X.-Q., Zhao, Y.-H., Chu, Y.-Q., et al. 2012, RAA, 12, 1197
Dehnen, W. 2000, AJ, 119, 800
Dehnen, W. 1998, AJ, 115, 2384
De Simone, R. S., Wu, X., & Tremaine, S. 2004, MNRAS, 350, 627
Famaey, B., Jorissen, A., Luri, X., et al. 2005, A&A, 430, 165
Faure, C., Siebert, A., & Famaey, B. 2014, MNRAS, 440, 2564
Gilmore, G., Wyse, R. F. G., & Norris, J. E. 2002, ApJL, 574, L39
Helmi, A., Navarro, J. F., Nordström, B., et al. 2006, MNRAS, 365, 1309
Høg, E., Fabricius, C., Makarov, V. V., et al. 2000, A&A, 355, L27
Holmberg, J., Nordström, B., & Andersen, J. 2009, A&A, 501, 941
Humphreys, R. M., Beers, T. C., Cabanela, J. E., et al. 2011, AJ, 141, 131
Jayaraman, A., Gilmore, G., Wyse, R. F. G., Norris, J. E., & Belokurov, V. 2013, MNRAS, 431, 930
Jurić, M., Ivezić, Z., Brooks, A., et al. 2008, ApJ, 673, 864
Kalnajs, A. J. 1991, in Dynamics of Disk Galaxies, ed. B. Sundelius (Goteborg: Goteborg Univ.), 323
Kordopatis, G., Recio-Blanco, A., de Laverny, P., et al. 2011, A&A, 535, A106
Kordopatis, G., Gilmore, G., Wyse, R. F. G., et al. 2013a, MNRAS, 436, 3231
Kordopatis, G., Gilmore, G., Steinmetz, M., et al. 2013b, AJ, 146, 134
Kordopatis, G., Hill, V., Irwin, M., et al. 2013c, A&A, 555, A12
Matijevič, G., Zwitter, T., Bienaymé, O., et al. 2012, ApJS, 200, 14
McMillan, P. J. 2011, MNRAS, 418, 1565
Minchev, I., Quillen, A. C., Williams, M., et al. 2009, MNRAS, 396, L56
Monari, G. 2014, PhD thesis, Univ. Groningen
Monari, G., Antoja, T., & Helmi, A. 2013, arXiv:1306.2632
Navarro, J. F., Helmi, A., & Freeman, K. C. 2004, ApJL, 601, L43
Perryman, M. A. C., Lindegren, L., Kovalevsky, J., et al. 1997, A&A, 323, L49
Reid, M. J., & Brunthaler, A. 2004, ApJ, 616, 872
Reid, M. J., Menten, K. M., Brunthaler, A., et al. 2014, ApJ, 783, 130
Robin, A. C., Reylé, C., Derrière, S., & Picaud, S. 2003, A&A, 409, 523
Roeser, S., Demleitner, M., & Schilbach, E. 2010, AJ, 139, 2440
Scargle, J. D., Norris, J. P., Jackson, B., & Chiang, J. 2013, ApJ, 764, 167
Schönrich, R., Binney, J., & Dehnen, W. 2010, MNRAS, 403, 1829
Sellwood, J. A. 2010, MNRAS, 409, 145
Sharma, S., Bland-Hawthorn, J., Binney, J., et al. 2014, ApJ, 793, 51
Siebert, A., Williams, M. E. K., Siviero, A., et al. 2011, AJ, 141, 187
Silverman, B. W. 1986, Density Estimation for Statistics and Data Analysis (London: Chapman and Hall)
Solway, M., Sellwood, J. A., & Schönrich, R. 2012, MNRAS, 422, 1363
Steinmetz, M., Zwitter, T., Siebert, A., et al. 2006, AJ, 132, 1645
VanderPlas, J., Connolly, A. J., Ivezic, Z., & Gray, A. 2012, in Proc. CIDU, ed. K. Das, N. V. Chawla, & A. N. Srivastava (Los Alamitos, CA: IEEE), 47
Williams, M. E. K., Freeman, K. C., Helmi, A. & the RAVE collaboration 2009 in IAU Symp. 254, The Galaxy Disk in Cosmological Context, ed. J. Andersen, J. Bland-Hawthorn, & B. Nordström (Cambridge: Cambridge Univ. Press), 139
Williams, M. E. K., Steinmetz, M., Binney, J., et al. 2013, MNRAS, 436, 101
Yanny, B., Rockosi, C., Newberg, H. J., et al. 2009, AJ, 137, 4377
Zacharias, N., Finch, C. T., Girard, T. M., et al. 2013, AJ, 145, 44
Zacharias, N., Finch, C., Girard, T., et al. 2010, AJ, 139, 2184